Bulletin of Glaciological Research 36 (2018) *15–22*
doi: 10.5331/bgr.18R01

Field activities at the SIGMA-A site, northwestern Greenland Ice Sheet, 2017

Sumito MATOBA[1*], Masashi NIWANO[2], Tomonori TANIKAWA[2], Yoshinori IIZUKA[1], Tetsuhide YAMASAKI[3,4], Yutaka KUROSAKI[1,5], Teruo AOKI[6], Akihiro HASHIMOTO[2], Masahiro HOSAKA[2] and Shin SUGIYAMA[1]

1 Institute of Low Temperature Science, Hokkaido University, Sapporo 060–0819, Japan
* matoba@pop.lowtem.hokudai.ac.jp
2 Meteorological Research Institute, Japan Meteorological Agency, Tsukuba 305–0052, Japan
3 Avangnaq, Takatsuki 596–0094, Japan
4 Institute of Arctic Observation Support, Yokohama 224–0006, Japan
5 Graduate School of Environmental Science, Hokkaido University, Sapporo 060–0810, Japan
6 Graduate School of Natural Science and Technology, Okayama University, Okayama 700–8530, Japan

(Received March 2, 2018; Revised manuscript accepted April 23, 2018)

Abstract

During spring 2017, we conducted research expeditions to the SIGMA-A site, which is located on the northwestern Greenland Ice Sheet. We maintained an automated weather station (AWS) to enable continuous meteorological observations. We extended 1.5-m long poles of the AWS and replaced two aerovane sensors, two thermo-hydrometers and an ultrasonic snow gauge. We also drilled an ice core and recovered a core with a total length of 60.06 m, conducted stratigraphic observations, and measured the density of the ice core. In addition, we conducted snow-pit observations and snow sampling, measured the specific surface area of snow using near-infrared reflectance, performed sunphotometry observations, and measured the spectral albedo. To schedule research activities in the field camp and helicopter pick-up flights, we received weather forecasts from the Meteorological Research Institute of Japan through the Internet using a satellite phone every day. We took a male dog to the field camp to alert us to approaching animals.

Key words: Greenland Ice Sheet, automated weather station, ice core, SIGMA-A, Qaanaaq

1. Introduction

The Greenland Ice Sheet (GrIS) has been losing mass at an accelerating rate since the 1990 s (*e.g.*, Rignot *et al.*, 2011; Shepherd *et al.*, 2012). Remote-sensing and numerical modeling studies indicate that the current loss of mass of the GrIS is caused by an increase in surface melt and ice discharge from marine-terminating outlet glaciers (van den Broeke *et al.*, 2009; Sasgen *et al.*, 2012; Enderlin *et al.*, 2014; Khan *et al.*, 2014). One of the underlying causes of this loss is the increasing air temperature, so-called global warming. However, we need to investigate a number of uncertainties to elucidate the mechanisms causing the GrIS to lose mass due to global warming, for instance, the reduction in the surface albedo of the GrIS, which is caused by pollution of the snow surface by light-absorbing impurities, such as soot or mineral dust, and microbial activities in the snowpack. This reduction in the albedo of the GrIS surface was detected by remote sensing studies (Box *et al.*, 2012).

The Snow Impurity and Glacial Microbe effects on abrupt warming in the Arctic project (SIGMA) established an observation site on the northwestern Greenland Ice Sheet (SIGMA-A site) and installed an automated weather station (AWS) in 2012 to investigate the processes causing the northwestern GrIS to lose mass. Project participants conducted meteorological and glaciological observations from 2012 to 2014 (*e.g.* Aoki *et al.*, 2014a; Yamaguchi *et al.*, 2014). Several interesting papers have been published using data obtained at the SIGMA-A site. Niwano *et al.* (2015) used in situ atmospheric and snow measurements to determine that low-level clouds accompanied by a significant temperature increase played an important role in an extreme snow melt event on the Greenland Ice Sheet, observed at SIGMA-A. They also modeled the extreme snow melt event numerically using a one-dimensional multi-layered physical snowpack model, the Snow Metamorphism and Albedo Process model (SMAP; Niwano *et al.*, 2012, 2014, 2018). Hori *et al.* (2014) found that thermal infrared remote sensing not only has the potential to supplement the shortwave infrared method for assessing surface snow types in the daytime but could serve as the only method for simultaneously retrieving both the snow type and surface temperature at nighttime, using the results of in situ measurements of

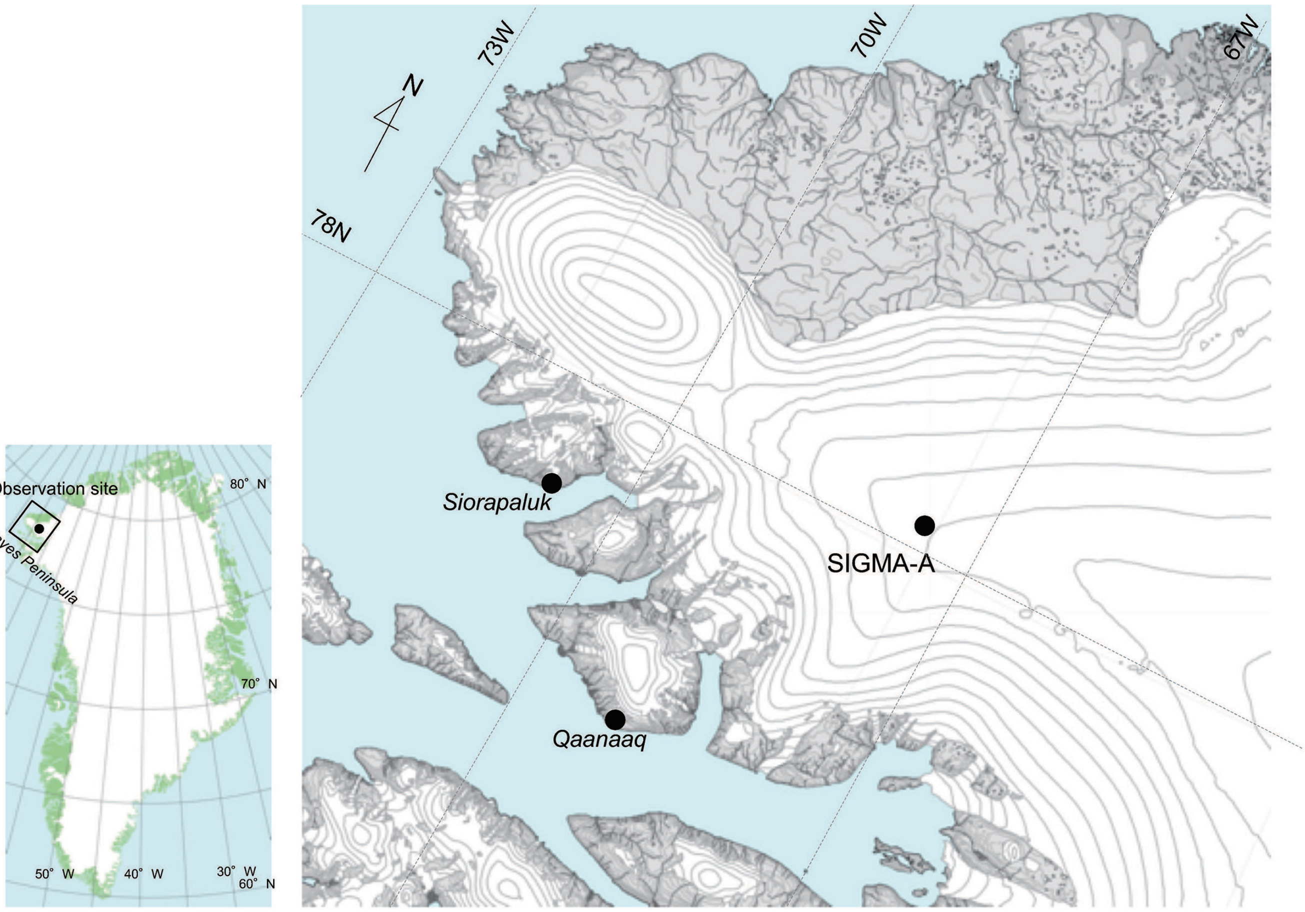

Fig. 1. Location of the SIGMA-A site (78°03′06″N, 67°37′42″W, 1490 m a.s.l.). The contour interval is 100 m.

the snow type and grain size as physical parameters to represent the state of the snow. These values were obtained from observations of the snow, various meteorological and optical parameters measured by AWS instruments, and whole-sky images taken with a sky-camera system (Aoki *et al.*, 2014a). Tanikawa *et al.* (2014) reported that the degree of polarization of the near-infrared reflected irradiance from the snow surface depended on the grain size of the surface snow, determined using data from field measurements at SIGMA-A and a flat field in Hokkaido, Japan. Aoki *et al.* (2014b) attributed the increase in the concentration of impurities (elemental carbon, organic carbon, and mineral dust) on the snow surface to the effects of sublimation/evaporation and snow melt amplification associated with the drastic surface melting of the Greenland Ice Sheet observed at SIGMA-A site in 2012.

We conducted our first research expedition to the SIGMA-A site since 2014 from 22 May to 6 June 2017. In this report, we summarize our field activities and the preliminary results of our expedition. The research expedition was conducted as part of the SIGMA-II Project, the Arctic Challenge for Sustainability (ArCS) project, and the Experimental Research Fund for Global Environment Conservation, funded by the Ministry of the Environment, Government of Japan.

2. Research Area

The SIGMA-A observation site (78°03′06″N, 67°37′42″W, 1490 m a.s.l.) is located 70 km northeast of the town of Qaanaaq in northwestern Greenland, and lies on the ridge of the Hayes Peninsula, which is north of Qaanaaq (Aoki *et al.*, 2014a) (Fig. 1). The SIGMA-A site is in an accumulation area, and the average annual surface mass balance was 0.27 m w. eq. yr^{-1} between 1975 and 2010. This value was estimated based on analyses of a 19-m-long ice core drilled in 2012 (Matoba *et al.*, 2016; Yamaguchi *et al.*, 2014).

3. Participants

This project was launched as a collaborative program between the SIGMA-II project, ArCS, and the Experimental Research Fund for Global Environment Conservation, which is supported by the Japanese Ministry of the Environment. The project participants were as follows:

Dr. Sumito Matoba (Institute of Low Temperature Science, Hokkaido Univ.), leader and ice core drilling.

Dr. Masashi Niwano (Meteorological Research Institute), AWS maintenance, spectral albedo measurements.

Dr. Tomonori Tanikawa (Meteorological Research

Institute), AWS maintenance, sun-photometric measurements, and observations of the optical properties of the snow pack.
Dr. Yoshinori Iizuka (Institute of Low Temperature Science, Hokkaido Univ.), ice core drilling and analyses, snow observations.
Mr. Tetsuhide Yamasaki (Avangnaq/Institute of Arctic Observation Support), chief of logistics and safety management.
Mr. Yutaka Kurosaki (Hokkaido Univ.), ice core drilling and analyses; snow observations.
Dr. Teruo Aoki (Okayama Univ.), ground support in Japan and Qaanaaq.
Dr. Masahiro Hosaka and Dr. Akihiko Hashimoto (Meteorological Research Institute), ground support in Japan

4. Itinerary

We chartered a Bell 212 Twin Huey (Bell, United States) helicopter from Air Greenland at Thule Air Base to fly personnel and equipment from Qaanaaq to the SIGMA-A observation site. The total weight of the equipment was approximately 900 kg, the volume of gasoline for the generator was 110 L, and the volume of kerosene for cooking and heating in the kitchen tent was 80 L. Two flights were required to transport all six personnel, the equipment, food, fuel, and a dog. We set up our camp on 22 May and stayed until 6 June. Our camp included a drilling tent, kitchen tent, six sleeping tents, a toilet tent, a snowpack observation trench, and a trench for taking spectral albedo measurements. All scheduled field studies were accomplished by 5 June. On 6 June, we flew all personnel, equipment, ice and snow samples, and the dog from the observation site to Qaanaaq over the course of two flights on a Bell 212. Snow and ice samples were stored temporally in a freezer, in which the temperature was maintained below −20℃, in the Pilersuisoq store in Qaanaaq. The snow and ice samples were then transported by a 20-foot reefer, in which the temperature was maintained below −20℃, on a Royal Arctic Line A/S vessel (Malik Arctica) from Qaanaaq to Aalborg in Denmark, and then by a 40-foot reefer, in which the temperature was maintained below −20℃, on a vessel from Aalborg to the Institute of Low Temperature Science, Hokkaido University, via Tomakomai in Hokkaido on 7 November 2017. The Institute of Arctic Observation Support oversaw the transportation of the snow and ice samples.

5. Field activities

5.1 AWS maintenance

An AWS was installed at the SIGMA-A site in June 2012. The AWS comprises a main pole that measures the air temperature, relative humidity, wind speed and direction, snow height change (by determining the distance between the snow surface and the sensor of an ultrasonic snow gauge), air pressure, tilt angle of the main pole, and snow temperature, and two sub-poles that measure short wave, long wave, and near infrared radiation (Aoki *et al.*, 2014a). Because the SIGMA-A site is located in an accumulation zone and snow height increases year by year, the AWS poles need to be extended every few years. We last extended these poles by 1.5 m in July 2014. On 23 May 2017, we again extended the poles and replaced several sensors for meteorological measurements, as follows. We made a 4-m long tripod with aluminum poles and hung a chain block from the top. We removed the main pole of the AWS by pulling its second arm by the chain block from a joint near the snow surface and placed the divided upper part of the main pole next to the divided lower part of the main pole. Then, we used drag ropes to pull the main pole down by hand. We replaced two aerovanes, two thermo-hydrometers, and an ultrasonic snow gauge. We also replaced a battery box containing eight cyclone batteries. After confirming that the replaced sensors functioned properly, we connected an extension to the main pole at the bottom of the AWS. We temporarily reduced the total weight of the AWS by removing the data logger from the main pole. We raised the divided upper part of the main pole manually, hoisted the upper part of the main pole with a chain block hung at the top of the tripod, and then joined the upper part to the lower part and immediately fixed the stays. To prevent the stays from being lost during the next melt season, we planted anchors for the stays at a depth of more than 1.5 m. On 5 June, the heights of the upper and lower arms of the AWS were 6.13 m and 3.13 m, respectively (Fig. 2).

Fig. 2. Main pole of the automated weather station at the SIGMA-A site, which we rebuilt.

We extended the sub-poles used to measure short-wave, long-wave, and near-infrared radiation by removing the poles by hand, joining them to the extension poles, replacing the cables, and re-installing them. We fixed the stays for the poles after adjusting the sensors

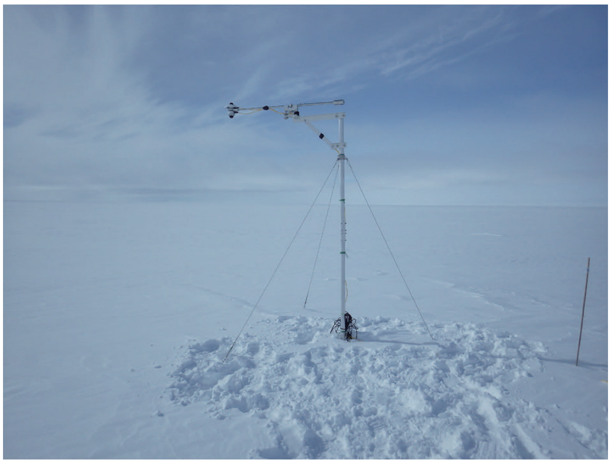

Fig. 3. Sub pole of the automatic weather station, used to measure near-infrared radiation.

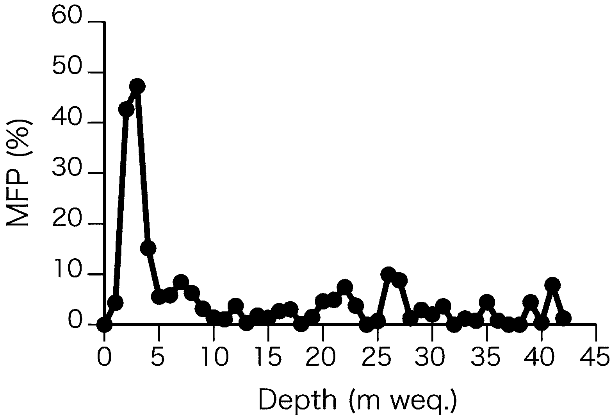

Fig. 4. Vertical profile of the melt feature percentage (MFP). We measured the MFP by measuring the thickness of the frozen ice layer from a 0.1-m w. eq. section of the ice core.

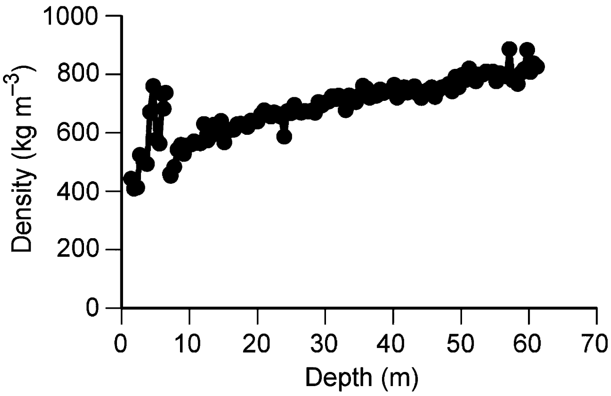

Fig. 5. Vertical profile of ice core density.

horizontally. These sensors were at a height of 2.38 m on 5 June (Fig. 3).

After fixing some problems with the AWS, such as a misconnected cable and a blown fuse in the hydro-thermometer, we confirmed that all of the correct data were being sent to Japan via the Argos satellite.

5.2 Ice-core drilling and processing

Having established the drilling tent and drilling facilities, we began drilling the ice core on 23 May. We completed drilling on 28 May. We used a light-weight electromechanical ice core drilling system developed by the technical division of the Institute of Low Temperature Science, Hokkaido University, for use at high elevations (Shiraiwa *et al.*, 2004; Matoba *et al.*, 2014; Iizuka *et al.*, 2016, 2017, 2018; Furukawa *et al.*, 2017). The total weight of the drilling system, which comprised a drive part, a chip chamber, a drill barrel, a controller, and a winch with armored cable, was approximately 100 kg. We used a single-barrel drill with a three pantographic-type anti-torque device and a half-round pulley on the top of the mast. We separated the core barrel into two parts, a chip chamber and core-storage space, because the drill system was easier to carry at a shorter length. We used a generator (a HONDA model EU16i) with a four-cycle, single-cylinder gasoline engine for the drilling operations. On 28 May, after 125 completed drilling runs, we finished drilling the ice core to a depth of 60.06 m.

We recorded the positions of ice layers observed in the ice core. Figure 4 shows a vertical profile of the melt feature percentage (MFP), which is the thickness of the ice layers in a section of the ice core 0.1 m w.eq. The MFP increased as the depth increased to above 10 m. We also measured the diameter, length, and weight of each ice-core segment to calculate its density (Fig. 5). The water-equivalent depth at the bottom of the 60.06 m ice core was 41.54 m w. eq.

The ice-core samples were placed in polyethylene bags and packed into insulated boxes without any cutting processes. They were then kept frozen during shipment to the Institute of Low Temperature Science in Japan.

5.3 Snow pit observations

On 30 May, we conducted snow-pit observations to a depth of 2.50 m. We measured the snow temperature, stratigraphy, and density (Fig. 6) and used stainless-steel tools to collect snow samples at 3-cm depth intervals. Each sample was placed in a separate polyethylene bag, and samples were kept frozen in the observation field so that the chemical composition of the ice could be analyzed at a later time.

We used the stratigraphy of the snow pack to estimate the ice forms in the layers at depths of 1.15–1.18, 1.46–1.51, and 1.770–1.775 m, corresponding to the melt layers from summer 2016, 2015/14, and 2013, respectively. The snow height change, as observed by the AWS, decreased between autumn 2014 and summer 2015 (Aoki *et al.*, 2017). Therefore, we assumed that the ice layer at 1.46–1.51 m depth, corresponding to the summer melt layer from 2015 and 2014, was relatively thick. The layers below a depth of 1.94 m were composed of hard melt forms and ice forms. The surface melt in 2012 is known to have been extreme (Niwano *et al.*, 2015), but that in 2011 was comparable to it. A snow pit observation at the

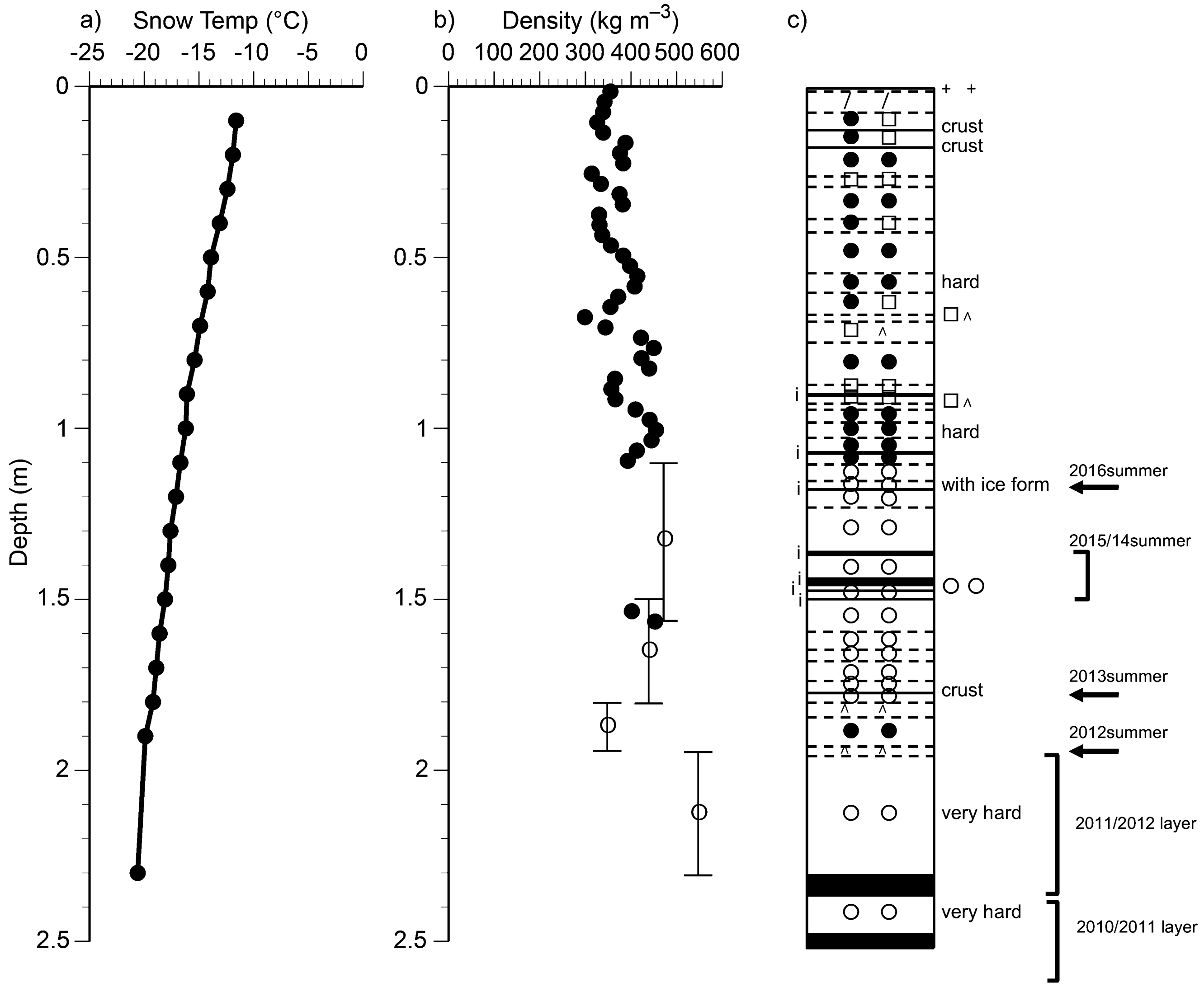

Fig. 6. Vertical profiles of snow temperature (a), snow density (b), and snow stratigraphy in the snow pit (c) on 30 May at the SIGMA-A site. The solid circle in (b) indicates the average snow density at 3 cm depth, centrally distributed from the center of the solid circle. The open circle indicates the average snow density of the snow/ice layer indicated by solid lines. The broken lines in (c) indicate the boundaries between the snow layers. The descriptions to the right of the figure showing the snow stratigraphy indicate the estimated ages of the snow layers.

SIGMA-A site in 2012 showed thick and hard ice layers below the snow layers (Yamaguchi *et al.*, 2014), and a snow pit observation near the SIGMA-A site at elevation 1469 m showed that the current snow layers were of the melt form and the temperature of the snow layer was 0℃ (Aoki *et al.*, 2014a). We considered that a hard melt form layer at 1.94–2.30 m was a refrozen layer that formed from the melt form snow layer during the 2012 melt season; that the ice form layer at 2.30–2.36 m, which formed in 2012, was superimposed on the hard melt form layer formed in 2011, which was a layer of refrozen melt snow; and that the ice layer below 2.45 m was a superimposed layer formed in 2011.

5.4 Snow sampling

When snowfall occurred, we collected fresh surface snow in polyethylene bags. The snow samples were then melted at ambient temperature and decanted into pre-cleaned polypropylene bottles at the windward side of the tent. This side was selected to prevent contamination by the generator exhaust and kitchen. The bottled samples were kept frozen in snow during the field observations and during their transport to Qaanaaq. They were stored at ambient temperature on the journey from Qaanaaq to the Institute of Low Temperature Science, Hokkaido University, where they were kept frozen in a cold laboratory until they were chemically analyzed.

We also collected snow blocks from the wall of the observation snow pit. The snow blocks were placed in polyethylene bags, packed into insulated boxes, and kept frozen until they were transported to the Institute of Low Temperature Science in Japan.

5.5 Measurement of the specific surface area (SSA) of snow using near-infrared reflectance

We determined the specific surface area (SSA) of the

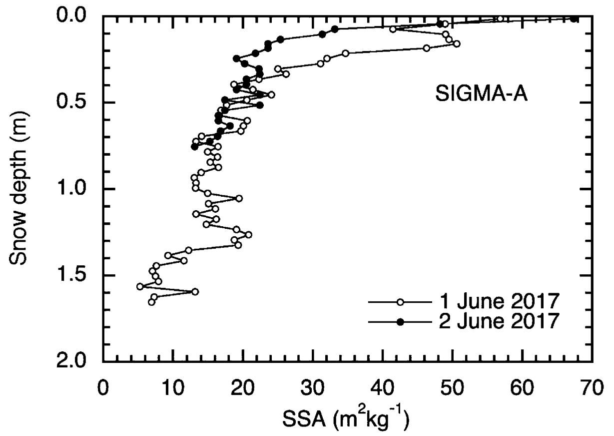

Fig. 7. Vertical profile of the specific surface area (SSA) of snow measured at SIGMA-A on 1 and 2 June 2017.

snow, a measure of the snow grain size, by measuring its near-infrared reflectance using a hand-held integrating sphere snow grain sizer (HISSGraS; Predo, Japan). These measurements were taken to enable evaluation of the vertical snow grain size profile, shown in Fig. 7, the temporal variations in the surface snow grain size, and the evolution of snow metamorphism. We also used these measurements to validate the snow grain size according to the satellite remote sensing method. The satellite validation measurements were synchronized with MODIS/Terra and Aqua overpasses.

5.6 Other observations

We also conducted sunphotometry observations to measure the optical depth of aerosols over the field site and the spectral albedo at the snow surface.

6. Safety management

6.1 Weather forecast for field activities and helicopter flights

Since 2012, personnel at the field camps at the SIGMA-A site have received weather forecasts from Japan using a satellite phone (Hashimoto *et al.*, 2016, 2017). The information is very important to the people conducting field activities at the camps and scheduling helicopter flights.

Information regarding the short-range and 7-day weather forecasts was sent to the field camp. The short-range weather forecast included details on the weather conditions, air temperature, wind speed and direction, and presence or absence of precipitation over the following 2 days. The short-range weather forecast was read from data predicted by the Japan Meteorological Agency Non-Hydrostatic Model (JMA-NHM, Saito *et al.*, 2006). The 7-day weather forecast included information regarding weather conditions and air temperature. The 7-day weather forecast was predicted based on the global forecast from the JMA Global Spectral Model (GSM) and 7-day weather forecasts from several websites, such as that of the Danish Meteorological Institute. The information was e-mailed from Japan at 7:00 local time (WGST; West Greenland Summer Time). Confirmations of the safety of the field camp, including a weather observation report, were e-mailed from the field camp to Japan at 19:00 WGST. The e-mails from Japan were received by a Google Gmail account and viewed in basic HTML on a browser (Microsoft Internet Explorer) on a notebook PC (Windows 7, 64 bit) connected to the internet using an Iridium satellite phone (model 9555) as a modem and Iridium Direct Internet software. Until 2014, we used a mailer (Thunderbird) on the same notebook PC to receive e-mails from a Gmail server via the Iridium satellite phone. Although the internet connection speed was the same, the mailer did not always receive complete e-mails. The mailer's settings caused it to cut the connection to the mail server when the connection time exceeded a time limit set by the mailer; this time limit could not be changed manually. If the connection to the mail server was cut, the mailer read e-mails from the server from the start. Therefore, it occasionally took more than 30 minutes to receive an e-mail. We used webmail systems instead of mailers during the field expedition described here. The volume of each e-mail sent by the webmail system was larger than the volume sent by the mailer. However, the system was better at receiving e-mails, and there was a large reduction in the total communication volume and time. Sometimes, messages were sent to members of the expedition from their families alongside the weather forecast. These were delightful to us and helped maintain our mental condition.

6.2 Caution against polar bears

Several residents of the Qaanaaq region said that many wolves had recently crossed the narrow strait from Canada to Inglefield and that muskox and reindeer, which had lived in Ingrefield, were moving southward to escape the wolves. Hence, the polar bears living near Inglefield were also are moving southward to hunt the muskox and reindeer, significantly increasing the risk that we might encounter polar bears at our field camp. Although we had taken a rifle on previous field expeditions, we had not taken any warning devices to alert us to animals approaching. On this field expedition, we took a male dog from Qaanaaq to alert us if polar bears approached the camp (Fig. 8). Fortunately, we encountered no polar bears, and the dog enabled us to have peaceful nights and kept us safe.

7. Concluding remarks

We conducted a research expedition to the SIGMA-A site on the northwestern Greenland Ice Sheet, where the SIGMA project established a research site in 2012. We extended the poles on the AWS and replaced the sensors of two aerovanes, two thermo-humidity meters, and an

Fig. 8. Photograph of the dog who prevented access to our field camp by polar bears.

ultrasonic snow gauge. We intend for meteorological data to be recorded by the AWS systems continuously over the next five seasons. To ensure this outcome, we will need to extend the AWS poles again within 3 years.

We obtained a 60.06-m-long ice core, from which we can recover data spanning 150 years. We are analyzing the physical properties of the ice core by taking detailed density measurements using x-ray and near-infrared spectrometry, as well as its chemical composition in terms of water stable isotopes and major ions.

Acknowledgments

We thank Air Greenland A/S and their Bell 212 pilot, Gear Paulsen, for supporting our flight operations and Sakiko Daorana, Navarana K'avigak, Toku Oshima, Kim Petersen, and Sofie Jensen for their logistical support in Qaanaaq. We also thank Hiroshi Utsumi of the Institute of Arctic Observation Support, Koichi Seki of Toyo Trans, and Daiki Sakakibara of Hokkaido University for transporting the ice core and equipment. The map shown in Fig. 1 is created by Nuna GIS (http://en.nunagis.gl/) operated by Asiaq, Greenland Survey. This study was supported in part by (1) JSPS KAKENHI Grant Numbers JP16H01772 and JP15H01733; (2) the Arctic Challenge for Sustainability Project (ArCS); (3) the Experimental Research Fund for Global Environment Conservation, Ministry of the Environment, Japan; (4) a grant from the Joint Research Program of the Institute of Low Temperature Science, Hokkaido University; and the (5) Okhotsk Network Program from the Pan-Okhotsk Research Center, Institute of Low Temperature Science, Hokkaido University.

References

Aoki, T., Matoba, S., Uetake, J., Takeuchi, N. and Motoyama, H. (2014a): Field activities of the “Snow Impurity and Glacial Microbe effects on abrupt warming in the Arctic” (SIGMA) Project in Greenland in 2011–2013. *Bull. Glaciol. Res.*, **32**, 3–20, doi: 10.5331/bgr.32.3.

Aoki, T., Matoba, S., Yamaguchi, S., Tanikawa, T., Niwano, M., Kuchiki, K., Adachi, K., Uetake, J., Motoyama, H. and Hori, M. (2014b): Light-absorbing snow impurity concentrations measured on Northwest Greenland ice sheet in 2011 and 2012. *Bull. Glaciol. Res.*, **32**, 21–31, doi: 10.5331/bgr32.21.

Aoki, T., Niwano, M., Tomonori, T., Hashimoto, A., Matoba, S., Sugiyama, S., Takeuchi, N., Motoyama, H., Naoko, N., Uetake, J., Hori, M., Shimara, R., Yamaguchi, S., Fujita, K. and Yamasaki, T. (2017): Field observations in Greenland by “Snow Impurity and Glacial Microbe effects on abrupt warming in the Arctic” (SIGMA) Project (in Japanese). *Polar News (Kyokuchi)*, **53** (1), 34–40.

Box., J. E., Fettweis, X., Stoeve, J. C., Tedesco, M., Hall, D. K. and Steffen, K. (2012): Greenland ice sheet albedo feedback: thermodynamics and atmospheric drivers. *The Cryosphere*, **6**, 821–839, doi: 10.5194/ tc-6-821-2012.

Enderlin, E. M., Howat, I. M., Jeong, S., Noh, M-J., van Angelen, J. H. and van den Broeke, M. R. (2014): An improved mass budget for the Greenland ice sheet. *Geophys. Res. Lett.*, **41** (3), 866–872, doi: 10.1002/2013GL059010.

Furukawa, R., Uemura, R., Fujita, K., Sjolte, J., Yoshimura, K., Matoba, S. and Iizuka, Y. (2017). Seasonal scale dating of a shallow ice core from Greenland using oxygen isotope matching between data and simulation. *J. Geophys. Res.: Atmos.*, **122**, 10873–10887, doi: 10.1002/2017JD026716.

Hashimoto, A., Niwano, M. and Aoki, T. (2016): Numerical weather prediction supporting cryospheric field observation campaign on the Greenland Ice Sheet (in Japanese with English abstract and captions). *J. Jpn. Soc. Snow and Ice (Seppyo)*, **78**, 205–214.

Hashimoto, A., Niwano, M., Aoki, T., Tsutaki, S., Sugiyama, S., Yamasaki, T., Iizuka, Y. and Matoba, S. (2017): Numerical weather prediction system based on JMA-NHM for field observation campaigns on the Greenland ice sheet. *Low Tem. Sci.*, **75**, 91–104, doi: 10.14943/lowtemsci.75.91.

Hori, M., Aoki, T., Tanikawa, T., Kuchiki, K., Niwano, M., Yamaguchi, S. and Matoba, S. (2014): Dependence of thermal infrared emissive behaviors of snow cover on the surface snow type. *Bull. Glaciol. Res.*, **32**, 33–45, doi: 10.5331/ bgr32.33.

Iizuka, Y., Matoba, S., Yamasaki, T., Oyabu, I., Kadota, M. and Aoki, T. (2016): Glaciological and meteorological observations at the SE-Dome site, southeastern Greenland Ice Sheet. *Bull. Glaciol. Res.*, **34**, 1–10, doi: 10.5331/bgr.15R03

Iizuka, Y., Miyamoto, A., Hori, A., Matoba, S., Furukawa, R., Saito, T., Fujita, S., Hirabayashi, M., Yamaguchi, S., Fujita, K. and Takeuchi, N. (2017): A firn densification process in the high accumulation dome of southeastern Greenland. *Arctic, Antarctic, and Alpine Res.*, **49**, 13–27, doi: 10.1657/AAAR0016-034.

Iizuka, Y., Uemura, R., Fujita, K., Hattori, S., Seki, O., Miyamoto, C., Suzuki, T., Yoshida, N., Motoyama, H. and Matoba, S. (2018): A 60 year record of atmospheric aerosol depositions preserved in a high-accumulation dome ice core, Southeast Greenland. *J. Geophys. Res.: Atmos.*, **123**, 574–589, doi: 10.1002 /2017JD 026733.

Khan, S. A., Kjær, K. H., Bevis, M., Bamber, J. L., Wahr, J., Kjeldsen, K. K., Bjørk, A. A., Korsgaard, N. J., Stearns, L. A., van den Broeke, M. R., Liu, L., Larsen, N. K. and Muresan, I. S. (2014): Sustained mass loss of the northeast Greenland ice sheet triggered by regional warming. *Nat. Clim. Change*, **4** (4), 292–299, doi: 10.1038/ nclimate2161.

Matoba, S., Shimbori, K. and Shiraiwa, T. (2014): Alpine ice-core drilling in the North Pacific region. *Ann. Glaciol.*, **55** (68), 83–87, doi: 10.3189/2014AoG68A020.

Matoba, S., Yamaguchi, S., Tsushima, A., Aoki, T. and Sugiyama, S. (2016): Surface mass balance variations in a maritime area of the northwestern Greenland Ice Sheet (In Japanese with English abstract and figure caption). *Low Temperature Science*, **75**, 37–44, doi: 10.14943/lowtemsci.75.37.

Niwano, M., Aoki, T., Kuchiki, K., Hosaka, M. and Kodama, Y. (2012): Snow Metamorphism and Albedo Process (SMAP) model for climate studies: model validation using meteorological and snow impurity data measured at Sapporo, Japan, *J. Geophys. Res.: Earth Surf.*, **117**, F03008, doi: 10.1029/ 2011JF002239.

Niwano, M., Aoki, T., Kuchiki, K., Hosaka, M., Kodama, Y., Ymagaguchi, S., Motoyoshi, H. and Iwata, Y. (2014): Evaluation of updated physical snowpack model SMAP. *Bull. Glaciol. Res.*, **32**, 65–78, doi: 10.5331/bgr.32.65.

Niwano, M., Aoki, T., Matoba, S., Yamaguchi, S., Tanikawa, T., Kuchiki, K. and Motoyama, H. (2015): Numerical simulation of extreme snowmelt observed at the SIGMA-A site, northwest Greenland, during summer 2012. *The Cryosphere*, **9**, 971–988, doi: 10.5194/tc-9-971-2015.

Niwano, M., Aoki, T., Hashimoto, A., Matoba, S., Yamaguchi, S., Tanikawa, T., Fujita, K., Tsushima, A., Iizuka, Y., Shimada, R. and Hori M. (2018): NHM-SMAP: Spatially and temporally high resolution non-hydrostatic atmospheric model coupled with detailed snow process model for Greenland Ice Sheet. *The Cryosphere*, **12**, 635–655, doi: 10.5194/tc-12-635-2018.

Rignot, E., Velicogna, I., van den Broeke, M. R., Monaghan, A. and Lenaerts, J. (2011): Acceleration of the contribution of The Greenland and Antarctic ice sheets to sea level rise. *Geophys. Res. Lett.*, **38**, L05503, doi: 10.1029/2011GL046583.

Saito, K., Fujita, T., Yamada, Y., Ishida, J., Kumagai, Y., Aranami, K., Ohmori, S., Nagasawa, R., Kumagai, S., Muroi, C., Kato, T., Eito, H. and Yamazaki, Y. (2006): The operational JMA Nonhydrostatic Mesoscale Model. *Mon. Weather, Rev.*, **134**, 1266–1298, doi: 10.1175/mwr3120.1.

Sasgen, I., van den Broeke, M., Bamber, J. L., Rignot, E., Sørensen, L. S., Woulter, B., Martinec, Z., Velicogna, I. and Simonsen, S. B. (2012): Timing and origin of recent regional ice-mass loss in Greenland. *Earth Planet. Sci. Lett.*, **333–334**, 293–303, doi: 10.1016/j.epsl.2012.03.033.

Shepherd, A., Ivins, E. R., Geruo, A., Barletta, V. R., Bentley, M. J., Bettadpur, S., *et al.* (2012): A reconciled estimate of ice-sheet mass balance. *Science*, **338**, 1183–1189, doi: 10.1126/ science.1228102.

Shiraiwa, S., Kanamori, S., Benson, C. S., Solie, D. and Muravyev, Y. D. (2004): Shallow ice-core drilling at Mount Wrangell, Alaska. *Bull. Glaciol. Res.*, **21**, 71–77.

Tanikawa, T., Hori, M., Aoki, T., Hachikubo, A., Kuchiki, K., Niwano, M., Matoba, S., Yamaguchi, S. and Stamnes K. (2014): In situ measurements of polarization properties of snow surface under the Brewster geometry in Hokkaido, Japan, and northwest Greenland ice sheet. *J. Geophys. Res.: Atmos.*, **119**, 13946–13964, doi: 10.1002/2014JD022325.

van den Broeke, M., Bamber, J., Ettema, J., Rignot, E., Schrama, E., van de Berg, W. J., van Meijgaard, E., Velicogna, I. and Wouters, B. (2009): Partitioning recent Greenland mass loss. *Science*, **326**, 984–986, doi: 10.1126/science.1178176.

Yamaguchi, S., Matoba, S., Yamasaki, T., Tsushima, A., Niwano, M., Tanikawa, T. and Aoki, T. (2014): Glaciological observations in 2012 and 2013 at SIGMA-A site, Northwest Greenland. *Bull. Glaciol. Res.*, **32**, 95–105, doi: 10.5331/ bgr.32.95.